

Innovative design of experimental blade cascade model for in-depth analysis of stall flutter

Pavel ŠNÁBL^{1,2}*, Chandra Shekhar PRASAD¹, Pavel PROCHÁZKA¹, Luděk PEŠEK¹, Václav URUBA^{1,3}, and Vladislav SKÁLA¹

¹ Institute of Thermomechanics of the CAS, Department of Dynamics and Vibrations, Dolejškova 1402/5, Praha, 182 00, Czech Republic

² Czech Technical University in Prague, Department of Mechanics and Mechatronics, Technická 1902/4, Praha, 166 07, Czech Republic

³ University of West Bohemia, Department of Power System Engineering, Plzeň, 301 00, Czech Republic

Abstract. Stall flutter is a serious threat to the operational integrity in turbomachinery, particularly in the final stage rotors of steam turbines and in compressors. Although computer science has developed rapidly and much of the research can be carried out using numerical tools, the simulation of some phenomena, such as stall flutter, is still very challenging and needs to be supported by experimental data. This paper presents an innovative experimental linear blade cascade design with five prismatic blades with pitch degrees of freedom, designed to be operated in a low subsonic wind tunnel. The geometry of the blade cascade was chosen on the basis of the experimental and numerical tests to allow stall flutter initiation. New suspension, measurement and electromagnetic excitation systems were developed and experimentally tested to allow accurate measurement of aerodynamic damping during controlled flutter tests. The novelty of the experimental blade cascade is the possibility of single pulse excitation of the blades. The cascade can be brought to the edge of stability by adjusting the angle of attack and flow velocity, and then the pulse can be used to induce stall flutter. Measurement of both mechanical and flow characteristics, also demonstrated in this paper, will provide data for in-depth analysis of stall flutter initiation and propagation.

Keywords: blade cascade; aeroelasticity; stall flutter; wind tunnel testing.

1. INTRODUCTION

This paper presents an innovative design of a new experimental blade cascade for the study of flutter with flow separation at the blades, stall flutter, which is not yet fully understood. The cascade is operated at low subsonic flow conditions up to $Ma = 0.15$. It is designed as a linear cascade with five NACA 0010 prismatic blades capable of oscillating at amplitudes up to 8° and frequencies up to 60 Hz. The novelty is the possibility of bringing the blade cascade to the edge of stability and then triggering the stall flutter by pulse excitation of one of the blades. This allows the study of the stability limits and post-critical behaviour of the blade cascade under stall flutter conditions. The results are important for theoretical studies and validation of numerical methods.

In Section 2, the current needs in the field of turbine aeroelasticity are presented, followed by the state of the numerical tools for these very complex calculations. Although the numerical tools have developed rapidly in the last decades, experimental research is still needed to verify the numerical models and to further study the aeroelastic phenomena, especially stall flutter. Next, an overview of the development of blade cascade experiments in the world is presented, highlighting the advantages

and disadvantages of specific design features. The standard approaches to controlled flutter testing are then described, and finally the history of flutter experiments at the Institute of Thermomechanics is briefly mentioned. Section 2 provides the reader with the background information necessary to understand the actual cascade design.

Section 3 describes the actual design and development of the new blade cascade. First, the geometry had to be tested to allow flow separation at the blades; in the previous experimental setup, the blades were closer together and the accelerated flow in the channels prevented stall. Then all the major parts of the cascade had to be designed and tested to our requirements.

Some of the initial measured and evaluated results are shown in Section 4. The controlled flutter tests were carried out first to test the stability limits of the cascade for different flow and vibration conditions. The pulse excitation tests were then carried out. The cascade was set to the known stability limit and pulse excitation was then applied to one blade. The dynamic response of all the blades and the flow field were measured and evaluated. Amplitude, instantaneous frequency, inter-blade phase angle (IBPA), aerodynamic moments and other quantities can be obtained from the measured data. From the particle image velocimetry (PIV) measurements of the flow field, instantaneous velocity fields can be extracted and more advanced statistical analyses can be performed. The results shown in Section 4 confirm the expectations of the newly designed blade cascade that it is possible to induce stall flutter in the cascade and measure its development and propagation.

*e-mail: snabl@it.cas.cz

Manuscript submitted 2024-01-22, revised 2024-05-14, initially accepted for publication 2024-05-28, published in September 2024.

2. OVERVIEW OF THE SOLVED TOPIC

2.1. Aeroelasticity in turbomachinery

In today's world, where ecology and sustainable development are more important than ever, and where renewable energy sources account for a large percentage of the total electrical energy produced by power plants, one might think that research in the field of steam turbines is no longer necessary. However, turbomachinery engineers are faced with the challenge of designing turbines that will not run at full power all the time as in the past. Renewable energy sources are highly dependent on the weather, and energy storage is still very limited, so steam turbines need to be developed in such a way that they can serve as a stable base for the electrical grid, covering peaks in energy consumption and production from renewable sources. Turbines must therefore be designed to operate in many different regimes with different mass flows. To increase efficiency, turbine technology is being pushed to its current limits and larger turbines are being built.

In large steam turbines, the final stage blades are very long and have to be very slim and shroudless to minimise centrifugal forces, resulting in low natural frequencies and low structural damping. In this case, aeroelastic damping plays an important role in the dynamics of the final stage disc. Three major aeroelastic problems found in turbomachinery as described in [1] are forced response, non-synchronous vibration and flutter. Flutter is an unstable, self-excited vibration resulting from the coupling between structural vibrations and unsteady aerodynamic forces. If flutter were to occur in a steam turbine, the vibration amplitude would increase, the blades would be subjected to high cycle fatigue and could eventually fail. It is clear that this unstable behaviour must be avoided and predictions of flutter behaviour must be made at the design stage of the turbine.

2.2. Numerical investigation

In order to achieve the planned aerodynamic performance and ensure aeroelastic stability in a short time, a significant number of design iterations are required at the preliminary design stage. The design iterations are primarily aimed at optimising the blade geometry and achieving the optimum blade arrangement in the cascade array. For this reason, numerical tools are preferred over physical models at this stage to save both time and cost. Currently, fully or loosely coupled high to medium fidelity computational fluid dynamics-computational structural dynamics (CFD-CSD) numerical tools are used by industry and researchers [2,3]. The CFD-CSD models and their derivatives provide reasonably representative results [4]. The majority of numerical methods are based on the solution of the Euler and Navier-Stokes equations with different turbulence models [5–12]. Computer-based tools allow numerical methods to be considered as a priority, since they can replace expensive experimental tests and solve 2D [5–7] and 3D [8–12] problems independently of the flow conditions. The numerical methods can deal with both steady state and dynamic aeroelastic stability problems. However, the methods used to solve the problem of dynamic blade stability in the steady state cannot satisfactorily describe the aeroelastic phenomena, and simulations are mainly based on the Navier-Stokes

equations normalised by the Reynolds number [8]. The closed-form solution of this system of equations makes use of various turbulence models, such as RANS or URANS, or the more sophisticated models based on large eddy simulations (LES) [13] and derivatives of LES. Their large number implies that there is currently no one that could adequately describe the flow domain with flow separation on the blades. It should be noted that the reliability of the numerical results depends mainly on the choice of the computational mesh, which determines the area of blade-flow interaction. At present, static orthogonal meshes, as well as the complex adaptive meshes, are mainly used. However, such approaches cannot adequately characterise the curvilinear boundaries, or the reconstruction and coordination of flow and blade meshes cause great difficulties [14].

Furthermore, there are some researchers who have used direct numerical simulations (DNS) [15, 16] methods to simulate cascade flutter with a very high degree of accuracy, at least for the flow part. Although DNSs are the most accurate numerical methods, they are also the most computationally expensive, often requiring advanced computing hardware. This makes them less desirable for wide application in the research field. On the other hand, reduced order numerical models (ROM) have gained significant popularity in the recent past for turbomachinery blade flutter/aeroelastic simulation. The ROMs are a good compromise between speed and accuracy, therefore they are used by many researchers for both 2D and 3D blade cascade flutter simulations [3, 17–20]. Good reviews of the recent advances in various computational numerical methods and ROM for turbomachinery flutter/aeroelastic simulation are presented in [4] and [19] and readers are encouraged to read them.

Therefore, it is clear from the above that computer-based numerical models are a great tool for analysing turbomachinery flutter in an economical and efficient way. With the advancement of computer hardware, the numerical models are getting closer to represent the real complex physical phenomena involved in flutter when accurately modelled. Not only are they capable of representing and capturing the real physics, but they can also generate significant amount of data in post-processing for deep analysis of the problem. This amount of data is usually very difficult to measure during experiments due to lack of suitable sensors or inaccessibility of internal parts or high cost of physical setups. However, there are slight disadvantages of the computer-based numerical models – before being used for any analysis, most of the numerical models need to be validated against some form of experimental data or on benchmark test case data, and it is not uncommon that there are discrepancies between the numerical and experimental results [21]. Therefore, it can be said that numerical models will not completely replace actual physical experiments in the coming future, no matter how advanced the computational models are. Thus, the importance of good experimental methods in turbomachinery flutter/aeroelastic analysis will remain very relevant in the coming future.

2.3. Experimental research

One of the earliest thorough experimental investigations of blade cascade flutter was conducted in [22,23]. A compressor cascade with oscillating blades was tested under varying conditions in-

cluding free stream velocity, angle of attack (AOA) and IBPA. The findings demonstrated that IBPA, which characterises the mode shape of a running wave, is the most critical factor that determines the stability of an oscillating blade cascade. Later, in [24], standard configurations for compressor and turbine cascades were introduced, with experimental and predicted data provided as benchmark material for flutter prediction calculations.

To evaluate cascade stability, motion-induced controlled flutter is an optimal approach. In this test, blade motion is controlled by an external mechanism and it is possible to evaluate cascade stability under specified vibration and flow conditions. Many institutions have conducted extensive experimental research on controlled flutter in blade cascades over the past four decades. Prominent research institutions in the field include EPFL Lausanne [24, 25], KTH Stockholm [2], NASA Glenn Research Centre [26], Durham University [27], and other noteworthy institutions. The experimental research is ongoing, and some of the latest papers are [28–31].

The experiments differ in many aspects. The first is the cascade geometry. Since it would be extremely complicated to perform controlled flutter experiments on real turbomachines with rotating bladed wheels, some degree of simplification is always necessary. Some of the experiments, e.g. [2, 32], work with non-rotating annular cascades, which are close to the real geometry but very difficult and expensive to build. Also, the measurement methods on these cascades are limited. For this reason, most experimenters use so-called linear cascades, where the tip section of the bladed wheel is unrolled, creating a linear cascade with parallel prismatic blades. These experiments are further away from the real case, but the aeroelastic phenomena of the cascade are still present. In addition, the linear cascades allow the relatively simple use of flow visualisation techniques such as PIV and Schlieren imaging.

The next aspect is the flow conditions, which range from low subsonic to transonic and supersonic wind speeds. While low speed wind tunnels are common in laboratories, there are few facilities where the transonic and supersonic blade cascades can be tested.

The most important aspect of building a new cascade, however, is the mechanical one. Blade cascades for studying the flow field are rigid and do not need any moving parts. However, since flutter is a result of flow-structure interaction, moving blades are required. Two eigenmodes of the turbine or compressor blade play a role in cascade flutter: the first bending mode, which causes translational, i.e. plunge, motion of the blade tip, and the first torsional mode, which causes rotational, i.e. pitch, motion of the blade tip. While there are few researchers who have included both pitch and plunge motion in their experiments [29, 33–35], the more common practice is to use only pitch, e.g. [28], or only plunge motion, e.g. [36], due to the great complexity of experiments with combined motion.

The mechanical realisation of the excitation plays a huge role in the capabilities of the blade cascade. Controlled flutter experiments require one or more blades to oscillate at a specific frequency, amplitude and IBPA (if multiple blades are oscillating). As the blades are subjected to transient aerodynamic forces,

kinematic excitation of the blades is ideal to maintain harmonic motion. Cam and follower mechanisms, e.g. [31, 32, 36], or crank mechanisms, e.g. [27], are commonly used for kinematic excitation. The main advantage is the true kinematic excitation, the disadvantage is the difficulty in changing the parameters. To change the blade amplitude, the cam or the crankshaft must be changed, to change the IBPA of the blades, the cams must be physically set to this IBPA. In addition, all parts must be manufactured precisely in order to minimise free play in the mechanism.

The alternative to kinematic excitation is electromagnetic force excitation, e.g. [29, 33–35]. The great advantage is the variability of the parameters - amplitude, frequency, IBPA - which can all be changed via the control unit without any changes to the hardware. It is also easy to control both pitch and plunge motion. However, electromagnetic excitation has its limitations. The blades are mounted on elastic elements and both electromagnetic and aeroelastic forces act on the blade. So, for example, in a flutter case, if the strong aeroelastic forces excite the blade, it becomes very difficult to control the blade motion by electromagnetic forces.

The type of excitation must be carefully chosen based on the purpose of the blade cascade. If the main purpose of the cascade is to study controlled flutter with specified parameters, with major non-linearities in the flow such as stall or shock waves, it is better to use kinematic excitation. On the other hand, if the main objective is to study the flow-structure interaction in general, while varying many parameters, the electromagnetic force excitation comes in handy. It is also possible to study the unstable behaviour of the blade cascade, which dominates over the controlled motion when the excitation is switched off or after the blade stability has been compromised by a force pulse.

2.4. Theoretical background

According to [37], two controlled flutter testing approaches exist:

1. Aerodynamic influence coefficient (AIC) approach presented in [38]. This method uses a single oscillating blade and the principle of linear superposition of aerodynamic influence responses measured on all blades in a cascade. The influence is calculated both in terms of both magnitude and phase and the results can be used to estimate the aerodynamic damping for any IBPA.

The general equation describing the AIC approach for the harmonic motion of the reference blade $\bar{\alpha}e^{i\Omega t}$ with amplitude $\bar{\alpha}$ and angular frequency Ω in [38] is

$$C_\beta = \bar{\alpha} \left[C_0 + \sum_{l=1}^{\infty} (C_{-l}e^{il\beta} + C_l e^{-il\beta}) \right]. \quad (1)$$

The unsteady force on the reference blade C_β in infinite cascade with all of the blades oscillating with IBPA β and amplitude $\bar{\alpha}$ is approximated in equation (1) as a linear superposition of unsteady forces C_0 , C_{-l} and C_l measured on all blades when only the reference blade 0 oscillates with unit amplitude. The IBPA β is introduced in terms $e^{il\beta}$ and $e^{-il\beta}$.

In [38] it is also shown that the unsteady forces C_{-l} and C_l become very small for higher l , that is for the blades further from the reference blade. This suggests, that for stability assessment of the cascade, it should not be necessary to measure the forces on all blades, but to measure only the reference blade 0 and its two neighbours on each side, blades ± 1 and ± 2 .

For the finite cascade with five blades with pitching degree of freedom, the equation (1) can be rewritten as

$$M(\beta, t) = M_0(t) + \sum_{l=1}^2 \left[M_{-l} \left(t + \frac{l\beta}{\Omega} \right) + M_l \left(t - \frac{l\beta}{\Omega} \right) \right]. \quad (2)$$

$M(\beta, t)$ is the equivalent unsteady aerodynamic moment as if all blades were oscillating at IBPA β , $M_0(t)$, $M_{-l}(t)$ and $M_l(t)$ are the measured moments from the cascade blades. IBPA β is included as a time shift of the measured moments of the adjacent blades with respect to the oscillation frequency Ω .

2. Energy method [39] using the travelling wave mode (TWM) approach. As described in [40], this method assumes that aerodynamic forces have negligible effect on structural dynamics. In this case, the natural frequencies and eigenmodes of the system can be determined in advance. Then in experiments and simulations, all blades in a row oscillate at the same frequency and amplitude with prescribed IBPA and the unsteady force on the reference blade is measured directly. The work per cycle and the aerodynamic damping on the reference blade are then calculated.

The aerodynamic damping parameter Ξ for the cascade with pitching motion of the blades was defined as

$$\Xi = -\frac{W_C}{\pi \bar{\alpha}^2}, \quad (3)$$

where W_C is the work per cycle and $\bar{\alpha}$ is the pitch amplitude. The aerodynamic damping parameter can be normalised to dimensionless form according to [22].

The work per cycle of the pitching blade can be calculated as an integral over a time period of one cycle:

$$W_C = \int_0^{\frac{2\pi}{\Omega}} M(t) \frac{d\alpha(t)}{dt} dt. \quad (4)$$

where $M(t)$ is the moment acting on the blade and $\alpha(t)$ is the angular displacement of the blade.

The calculation of the aerodynamic damping parameter Ξ can be simplified for cases where both the measured moment $M(t)$ and displacement $\alpha(t)$ are sinusoidal, without solving the integral in equation (4):

$$\Xi = -\frac{\bar{M}}{\bar{\alpha}} \sin \phi_M = -\text{Im} \left(\frac{\mathcal{F}\{M(t)\}}{\mathcal{F}\{\alpha(t)\}} \Big|_{\frac{\Omega}{2\pi}} \right), \quad (5)$$

where \bar{M} is the moment amplitude and ϕ_M is the phase shift of the moment with respect to the angular displacement. \mathcal{F} denotes the Fourier transform. More details can be found in [42].

The unsteady moment $M_0(t)$ generated by the flow and acting on the oscillating reference blade cannot be easily measured in either AIC or TWM, because the measured signal also includes moments generated by the inertia I and damping D of the blade:

$$M_0^{Meas.}(t) = M_0(t) + I\ddot{\alpha}(t) + D\dot{\alpha}(t). \quad (6)$$

Two methods of extracting the unsteady aerodynamic moments from the measured signal, subtraction and identification methods, were used on the previous version of blade cascade and are described in [42]:

1. The subtraction method, which uses two measurements for each case, one with the flow and one without the flow. The measured moment without flow is then subtracted from the moment with flow to give the unsteady aerodynamic moment $M_0(t)$.
2. The identification method, which uses the measured data without the flow to identify the parameters I and D , which are then used to calculate the inertial and damping moments $I\ddot{\alpha}(t)$ and $D\dot{\alpha}(t)$ in equation (6).

Both of the above mentioned methods have their drawbacks, which are described in [43]. In that paper another method of evaluation was proposed. If the measured moment given by equation (6) is used directly to calculate the work per cycle using integral (4), then only the terms $M_0(t)$ and $D\dot{\alpha}(t)$ can contribute to the work. And if the cascade is designed so that the damping of the blade is very low, then the contribution of the damping term $D\dot{\alpha}(t)$ to the work is negligible.

2.5. Flutter experiments in the Institute of Thermomechanics of the CAS

The history of subsonic flutter studies at the Institute of Thermomechanics of the CAS (IT CAS) dates back to the year 2004, when an experimental rig for the study of airfoil flutter was built. The test rig, connected to a suction wind tunnel, was equipped with a single airfoil suspended from a mechanism that allowed pitch-plunge motion of the profile [44]. The airfoil was made hollow to allow the installation of pressure sensors and the addition of weights to change the centre of mass. The test section had transparent side walls for optical measurements (e.g. interferometry and Schlieren imaging) [45]. On this test rig, innovative measurement methods were tested, e.g. evaluation of unsteady force distribution along the self-oscillating airfoil from interferograms [46], dynamic behaviour of the fluttering blade such as stability at the onset of flutter was studied [47]. Later, the experimental rig was extended to accommodate a 5-blade cascade instead of a single profile [48]. In this cascade, each blade had its own pitch degree of freedom and there was a common plunge degree of freedom for all blades.

In [49, 50], a simplified cascade for studying classical flutter with three oscillating flat plates with only plunge degree of freedom (DOF) was used as a test case for the CFD solver FlowPro. To get closer to a bladed disc case, two more fixed flat plates

were later added [51], and an experimental setup of this cascade was built to verify the numerical results. The experimental results obtained from particle image velocimetry (PIV) shown in [52] prove that the aerodynamic coupling between the blades is insignificant with only the plunge DOF. To make the coupling more pronounced, the blade chord length was increased to create a greater overlap between the blades. The stability of the blade cascade was evaluated both experimentally and numerically, and although there was a decrease in the aerodynamic damping parameter for the backward running wave, the flutter instability was not reached; the cascade remained stable under all operating conditions [53].

As a next step, it was decided to build a 5-blade cascade with the same dimensions and pitch DOF of the blades to study stall flutter. Instead of flat plates, 3D printed symmetrical NACA 0010 profiles were used. The blade shafts were supported in ball bearings, free rotation of the blades was restricted by torsion springs, and excitation was provided by linear shakers of our own design. The motion of the shaker was transmitted via a piezoelectric force cell and then converted from linear to rotary via a rod and arm. A more detailed overview of the cascade design can be found in [54]. Controlled flutter experiments have been performed on this cascade and have shown flutter instabilities. Investigation of the flow field with PIV showed that there was no flow separation on the inner blades of the cascade and that the instability was of the classical flutter type. The experimental data were used to ROM in [18]. The design was easy to make, using conventional parts such as ball bearings and torsion springs, and instrumentation available in our institute. The cascade worked well for observing the flow field with or without forced harmonic excitation. However, measuring the aerodynamic moments through the force cell connecting the shaker to the rest of the mechanism proved almost impossible due to non-linearities and high damping. These unwanted effects were mainly caused by the ball bearings, friction between the coils of the torsion springs, free play in the connection of the rod to the arm, etc. The piezoelectric force cells used for measurement were small and lightweight, but had the disadvantage that they could only measure dynamic force, not static force.

Based on the experience gained from the previous experiments, it was decided to build a new, improved cascade, which is now the subject of this paper.

3. BLADE CASCADE DESIGN

3.1. General specification

Our research interest is the study of stall flutter at low subsonic flow speeds up to $Ma = 0.15$. The cascade is designed as a linear cascade with five NACA 0010 prismatic blades. All the blades are mounted on a rotating part that allows the AOA of the incoming flow on the cascade to be adjusted in the range $\pm 16^\circ$. We are mainly interested in the initiation and propagation of stall flutter in the cascade, but controlled flutter tests will also be carried out to assess the stability of the cascade under different flow and vibration conditions according to the theory described in Subsection 2.4.

Since stall flutter did not occur in the previous cascade due to stabilising effect of the accelerated flow in narrow inter-blade channels, simplified experiments with three blades and numerical studies with increasing blade spacing were carried out to achieve the flow separation at the centre blade of the cascade that is important for stall flutter instability. The dimensions set for the new cascade are shown in the schematic in Fig. 1a and the detail of the blade in Fig. 1b. The NACA 0010 profiles were generated for a chord length of $c_0 = 73$ mm and were shortened to $c = 70$ mm with a radius of 0.47 mm due to 3D printing not allowing a sharp trailing edge. The circular hole in the blade is for the shaft and corresponds to the axis of rotation, the rectangular hole is for the weight to balance the blade.

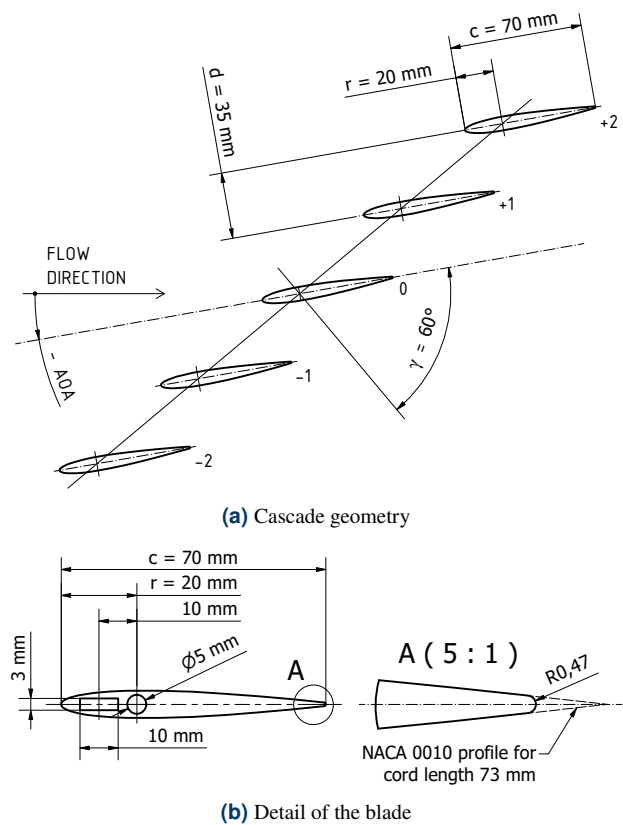


Fig. 1. Geometry of the new blade cascade

With the experience gained from previous experiments and by comparing the advantages and disadvantages of various design features found in the literature, it was decided to design a new blade suspension system and instrumentation with the following improvements:

- As ball bearings and torsion springs had proved unsuitable for this application due to significant non-linear damping, a flat spring suspension system was developed and tested.
- Torsional electrodynamic actuators were designed and used to excite the blades, eliminating the need for an additional transmission mechanism used in the previous cascade to connect linear electrodynamic shakers to the blades.
- The moment measuring shaft was used to connect the blade to the rest of the mechanism. Thus, all non-linearities and

damping in the suspension are separated by the moment sensor. During blade oscillation, in addition to the aerodynamic moment, only the blade inertia and damping (very small in this case) would be measured and it should be easily possible to subtract it.

3.2. Flat spring suspension system

The purpose of the suspension system is to elastically fix the blade in its axis of rotation to allow the pitch movement of the blade and to limit the movement in all other DOFs. In the new cascade design, the aim was to avoid bearings and wound torsion springs to reduce damping and non-linearities in the suspension system.

A flat spring suspension system has been developed to achieve this. It uses four thin flat sheets of spring stainless steel arranged in a cross. These sheets are clamped on one side to a part fixed to the frame and on the other side to a moving part connected to the moment measuring shaft, the torsion actuator coils and the blade. The flat spring suspension system prototype is shown in Fig. 2a. The design of the suspension element allows the stiffness to be varied by selecting different thicknesses of the flat springs.

To achieve low damping, the connection between the flat springs and the other parts must be as rigid as possible. For this reason, the attachment planes and special washers are designed so that only a thin strip near the edges clamps the flat spring. Details can be seen in Fig. 2b.

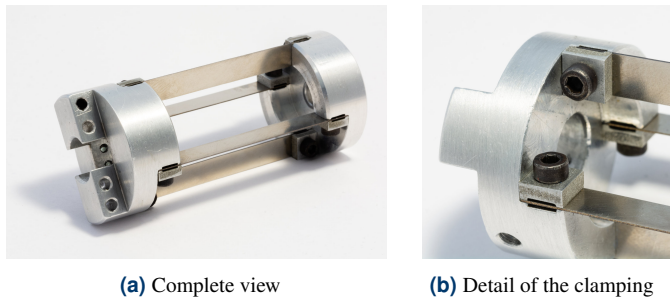


Fig. 2. Prototype of the flat spring suspension system

The stiffness characteristic of the suspension system was measured by applying a quasi-static moment to the moving side and measuring both the moment and the displacement with respect to the fixed part. The measured moment as a function of angular displacement is shown in Fig. 3. There is negligible hysteresis in the measured, meaning that the deformation of the suspension system can be considered purely elastic. The operating range of the suspension system is $\pm 9^\circ$ and thus the maximal amplitude of the blade should not exceed 8° to avoid hitting hard stops.

For small displacement angles up to 2° the characteristic is linear with constant stiffness. At larger angles the characteristic becomes non-linear due to increasing stiffness and can be approximated by the cubic equation

$$M = k_1\varphi + k_2\varphi^3, \quad (7)$$

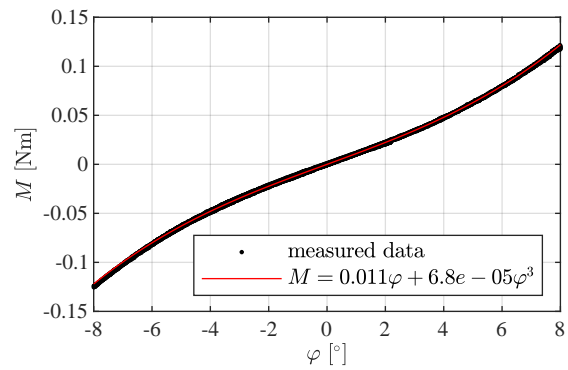


Fig. 3. Stiffness characteristic of the flat spring suspension system

where M and φ are the moment and the angular displacement, k_1 and k_2 are constants that can be obtained by curve fitting on the measured data. The fitted cubic equation can be also seen in Fig. 3. The stiffness characteristic is important in simulations of the cascade behaviour.

3.3. Torsion actuators

The previous cascade used linear shakers to excite the blades. However, this required an additional mechanism to drive the blades and the linear shakers had their own suspension springs. A better solution is to use actuators that drive the rotary motion directly, and such a commercial actuator was purchased to test this concept on our blade cascade. In addition, there is no mechanical connection between the static and moving parts of the actuator, so the actuation is essentially contactless.

The actuator has been tested on a single blade system and it was shown that it can easily excite the blade with harmonic motion in the desired frequency range of 10 Hz to 60 Hz. However, this actuator was too large and it wouldn't be possible to install more of them side by side to excite multiple blades. In addition, the arrangement of the actuator with one coil only creates not only a moment on the shaft but also a shifting force.

It was decided to design and build a similar actuator ourselves. We could place two coils opposite each other on the shaft to eliminate the shifting force and double the torque, and we could make the actuator smaller because we only needed a range of motion of about $\pm 5^\circ$. 3D printing technology was used to create the prototypes shown in Fig. 4. Each of the coils has 200 turns of 0.25 mm copper wire and the stator for each coil is fitted with two NdFeB magnets of dimensions $15 \times 10 \times 4$ mm with a magnetic force of 40 N. The prototypes have also been tested



Fig. 4. 3D printed prototypes of in-house built torsional excitation coils

on a single blade system and have proved to work without any problems.

3.4. Moment measuring shaft

Based on the maximum moment measured on the profile of the previous cascade and numerical simulations, we searched for moment sensors with load capacity of 0.1 Nm and small dimensions on the market. A suitable sensor was found and purchased. At the same time, a company which specializes in strain-gauge sensors was asked to produce moment measuring shaft with load capacity 0.1 Nm and same dimensions as the commercial one, so that we could use either of those sensors.

To test the performance, the sensors were connected in series, a periodic torque was applied and the responses of both sensors were observed on the oscilloscope. It was found that the signal from the off-the-shelf sensor was much noisier than that from the custom-built sensor, so it was decided to use the custom-built for the new cascade. Four more were made to equip all the blades.

3.5. Testing of new features on the previous blade cascade

The new blade assembly consists of the flat spring suspension, torsion shaker, moment measuring shaft, blade and miniature encoder. The blade and miniature contactless rotary encoder from the previous cascade were used. In order to test the new blade assembly on the previous cascade, an attachment was made using metal rods and 3D printed parts.

Initially, the torque shaft was calibrated by hanging weights on the leading and trailing edges of the blade and measuring the voltage from the strain gauge amplifiers. The calibration chart can be seen in Fig. 5. During calibration, when weights were hung on the blade, a non-negligible bending of the whole assembly was observed, although the suspension system is quite stiff in this direction. This is caused by the combined elasticity of the suspension system, the moment measuring shaft and the blade. The forces from the weights, which are comparable to the aerodynamic forces during the measurements, act on a long arm (the total distance from the tip of the blade to the fixed frame is 230 mm), which generates a large bending moment. In order to maintain only one degree of freedom of the blade, it is necessary to provide additional support at the tip of the blade. It was decided to use a miniature friction bearing from a tiny electric motor as a support because of its low resistance to movement,

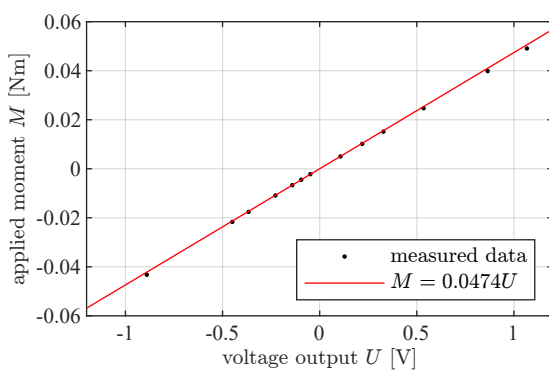


Fig. 5. Calibration chart of the moment measuring shaft

achieved by its small diameter (the one used for testing had a diameter of 1.5 mm) and precisely polished surfaces. Such a bearing will not significantly affect the damping of the blade, but it will ensure that the blade does not bend.

With this setup, several measurements were made using the AIC approach with only the reference blade oscillating. During the evaluation it was found that the encoder resolution of 0.09° was not sufficient to correctly evaluate the aerodynamic damping. A laser vibrometer was added to the measurement setup and aimed at the blade surface at a specified distance from the centre of rotation to measure the angular displacement simultaneously with the encoder. Fortunately, both approaches for assessing the stability of the cascade under controlled flutter, AIC and TWM, only require measurement of the motion of the reference blade, which can be measured by the laser vibrometer. For amplitude and IBPA control during TWM measurements, the encoder resolution is sufficient.

These first tests verified the whole concept and proved it to be fully functional with respect to the pros and cons of force excitation described in Subsection 2.3. The most problematic cases are those where the ratio between the aerodynamic forces and the excitation forces is high, causing non-sinusoidal blade motion or even self-excited flutter regardless of the excitation. These are typically low excitation frequency cases (low excitation forces due to low blade acceleration) or high AOA cases when the stall flutter starts. However, the disadvantages are outweighed by the advantages of rapid change of vibration parameters and pulse excitation. Pulse excitation is useful in cases where the blade cascade is close to the stability limit and the moment pulse can trigger the flutter.

3.6. Realisation of the new blade cascade

The complete experimental setup, consisting of the tunnel extension and the cascade itself, was manufactured by external companies. The finished cascade structure with the tunnel extension, needed to increase the height of the channel to accommodate five blades with increased blade spacing, can be seen in Fig. 6. The support structure holds circular rotating part that holds the blades and allows the AOA on the blades to be changed.

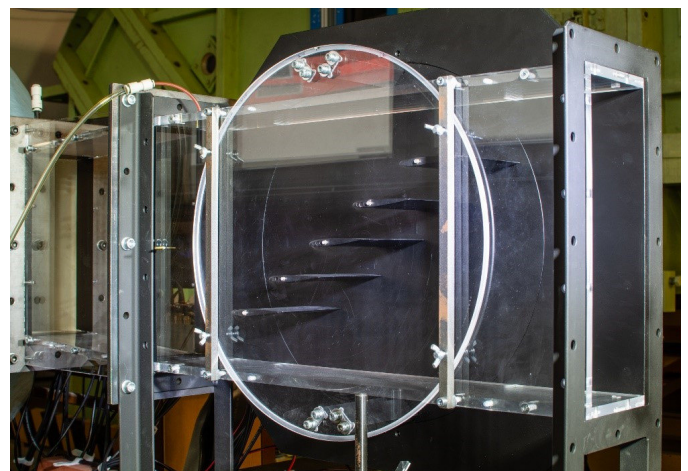


Fig. 6. View on the new blade cascade connected to the wind tunnel

Behind the metal side wall there is the assembly of all critical parts that were described above – flat spring suspension systems, torsion actuators and moment measuring shafts. The complete assembly of all five blades can be seen in Fig. 7.

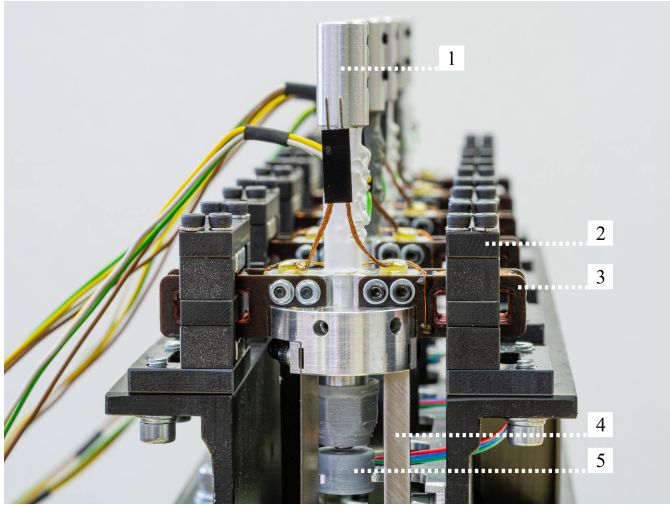


Fig. 7. Assembly of the blade cascade support, excitation and instrumentation. 1 – moment measuring shaft, 2 – excitation stator with permanent magnets, 3 – excitation coil, 4 – flat spring suspension, 5 – rotary encoder

Once the mechanical part of the cascade was built, the electrical part had to be solved. Encoders require a supply voltage and then produce an analogue signal directly. The strain gauges of the torque transducers have to be connected to a full bridge and to instrumentation amplifiers, which provide the supply voltage and amplify the strain gauge outputs. The torsion shakers are connected either to audio amplifiers if we want to provide harmonic excitation, or to the Institute's own amplifiers for pulse excitation. All measurement data is collected using a digital multi-channel signal recorder.

For the harmonic excitation, a closed-loop control system was implemented in real-time controller. The aim of the control system is to control the frequency, amplitude and IBPA of all the blades. While the frequency is directly given by the frequency of the sine wave sent to the amplifier, the amplitude and IBPA have to be fine-tuned to the desired values. There are several reasons for this. Many of the parts are handmade (blades, coils, etc.) and their mechanical properties, such as weight and inertia, and electrical properties, such as the impedance of the coils, vary in each blade subsystem. In addition, the blades are subject to moments generated by the flow, which also affect the amplitude and phase of the vibration.

The amplitude control is automatic - it uses the encoder signals in a feedback loop; the actual amplitude over several oscillation periods is observed, compared with the desired amplitude and the difference is sent to the PID controller with integral gain only. This keeps the amplitude constant regardless of flow conditions, oscillation frequency, etc.

A more difficult task is the IBPA control. In the real-time controller it was not possible to calculate the phase shift using FFT or Hilbert transform, so a root mean square (RMS) solution

was devised. Suppose the blades i and $i + 1$ are to oscillate with the desired IBPA β_D . The generated sinusoidal signals are $\alpha_i = \bar{\alpha} \sin(\omega t)$ and $\alpha_{i+1} = \bar{\alpha} \sin(\omega t - \beta_D)$ respectively. These signals are sent to the amplifiers and the blades start to oscillate with the actual IBPA $\beta_A \neq \beta_D$ due to the unequal mechanical and electrical properties mentioned above. The movement of the blades is measured with rotary encoders and sent to the control system where the measured signal of the blade $i + 1$ is shifted in time with $t_{shift} = \beta_D / \omega$, subtracted from the signal of the blade i and the RMS of the signal difference over a period of 1s is calculated. A time delay is manually added to the generated signal for blade $i + 1$ to minimise the value of the RMS and thus $\beta_A \rightarrow \beta_D$.

4. MEASUREMENT CAPABILITIES OF THE INNOVATIVE BLADE CASCADE

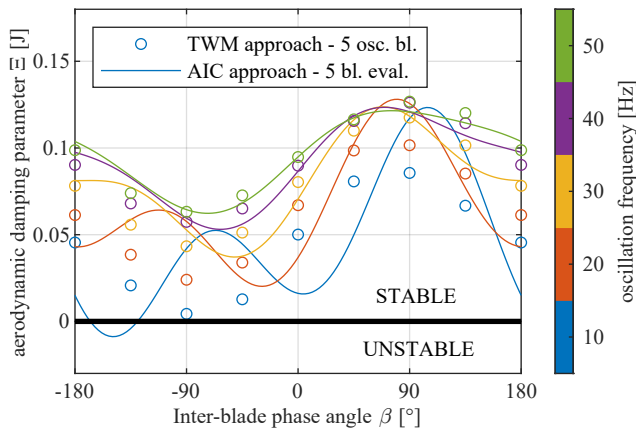
4.1. Controlled flutter testing with TWM and AIC approach

The TWM and AIC approaches were used to assess the stability of the blade cascade and the limitations of these test methods were compared. The TWM approach with harmonic force excitation of all five blades was tested first. At a wind speed of 20 ms^{-1} , the maximum negative AOA (see Fig. 1a) for which the force excitation was able to maintain the controlled motion was -6° . Further increases in negative AOA resulted in self-excited flutter. As an example, stability curves (S-curves) obtained from TWM measurements at 20 ms^{-1} , AOA -6° and oscillation frequencies from 10 to 50 Hz are shown as circles in Fig. 8. The results show that at the lowest frequency the stability parameter drops to zero for IBPA -90° and that increasing the oscillation frequency stabilises the cascade.

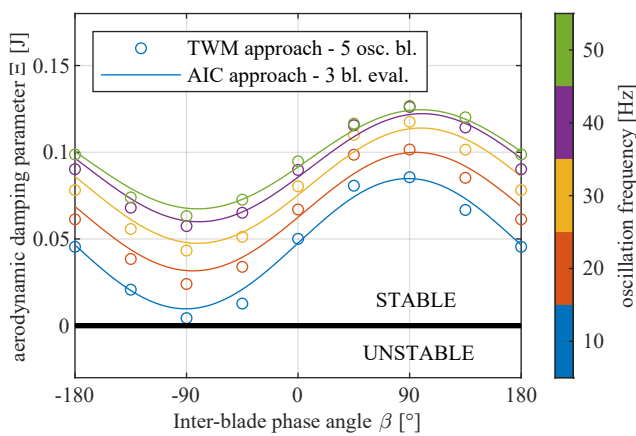
The AIC approach measurement was then performed using the same parameters and evaluated from the force responses measured on all five blades. The results are shown as lines in Fig. 8a. Whilst at higher frequencies the stability curves match well, at lower frequencies there is a strong influence from the ± 2 blades, causing the strong second harmonic of the stability curve over the IBPA according to equation (2). The limitation of the AIC approach here is that it was derived for an infinite blade cascade as described in Subsection 2.4, but our cascade consists of only 5 blades. Thus, blade -2 has no neighbour on its underside, resulting in flow separation under the blade even at small AOA. The moment variations measured at blade -2 are then dominated by the separated flow and not by the oscillation of blade 0. As it is known that the influence of the oscillating blade 0 on the blades further down the cascade decreases rapidly [38], we tried to evaluate the stability curves with the AIC approach considering only blade 0 and its direct neighbours, blades ± 1 . The results are shown in Fig. 8b and we see that the AIC results agree with the TWM results even at low frequencies. The small differences may be due either to neglecting the effect of blades ± 2 .

Both approaches have certain limitations with the new blade cascade. The TWM approach can only be used within the stability limits where it is possible to maintain the controlled oscillation of all blades. In the AIC approach it is not good to

Experimental blade cascade for analysis of stall flutter



(a) TWM with 5 oscillating blades and AIC with 5 measured blades



(b) TWM with 5 oscillating blades and AIC with 3 measured blades

Fig. 8. S-curves of the cascade at 20 ms^{-1} , $\text{AOA} -6^\circ$ and different oscillation frequencies

include the influence of blades ± 2 because these are the first and last blades and the periodicity of the cascade is violated there. However, the stability curves evaluated from the AIC approach without blades ± 2 show very good agreement with the TWM approach, meaning that the blade cascade is in the range of classical flutter with attached flow and the linear superposition principle is valid. Therefore, AIC can be used to evaluate the cascade stability. Using the AIC approach with only blade 0 oscillating, it is possible to achieve higher negative AOAs due to better resistance to self-excited flutter. In addition, the AIC approach makes it easier and quicker to obtain the stability curves, which may be useful for testing different blades in the future.

4.2. Pulse-triggered stall flutter testing

The main reason for using electromagnetic force excitation in the blade cascade is the ability to excite the blades with short moment pulses. When the blade cascade is brought to the edge of stability by wind speed and AOA, the pulse applied to one blade can trigger stall flutter of the entire blade cascade. Studying the onset of stall flutter provides valuable information about the behaviour of the non-linear aeroelastic coupling present in the system.

Such an experiment was carried out at wind speed 20 ms^{-1} and $\text{AOA} -8^\circ$. The blades ± 2 were fixed and a 5ms moment pulse was applied to blade -1 . The angular displacements of blades 0 and ± 1 are shown in Fig. 9a. The impulse at time 0 caused the angular displacement of blade -1 to reach 2° . This is followed by the onset of flutter where the amplitudes of all three compliant blades increase. After 1s the system reaches a steady state. The different amplitudes of the blades are caused by the non-uniform flow through the cascade due to the small number of blades and their arrangement in the channel. It is interesting to observe the instantaneous frequency during the onset of flutter, which has been evaluated by the Hilbert transform and is shown in Fig. 9b. The natural frequency of the blades is around 26Hz and this is also the frequency at which they start to oscillate shortly after the pulse. However, during the initial transient phase, the flutter frequency of all oscillating blades increases to around 28.5Hz. This increase is most likely due to the additional stiffness introduced by the aeroelastic coupling during the flutter.

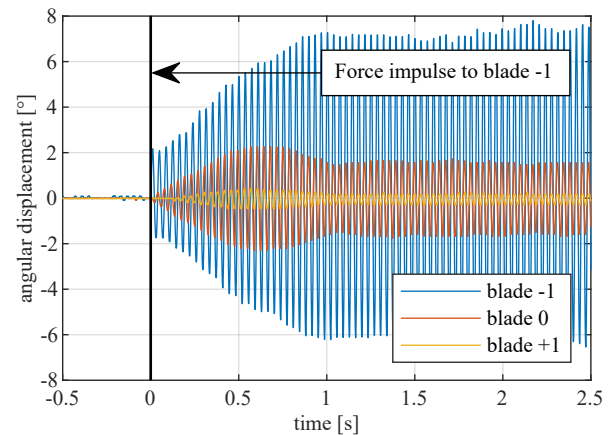
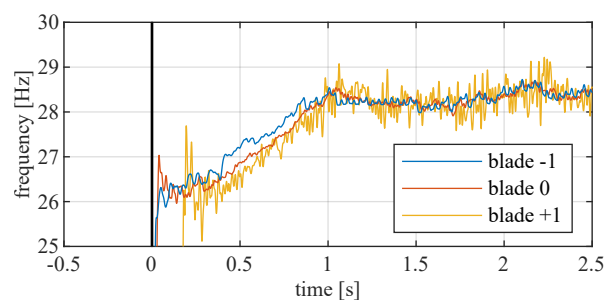
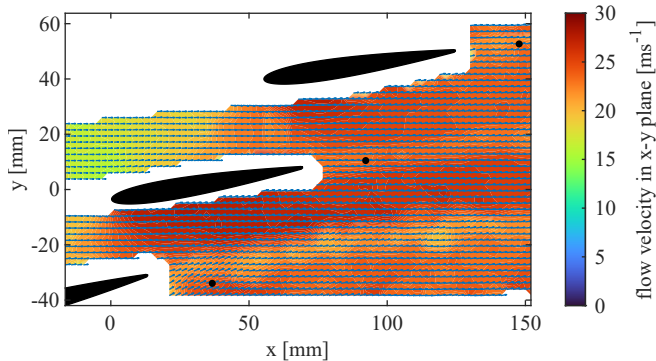
(a) Angular displacement of blades -1 , 0 and $+1$ (b) Instantaneous oscillation frequency of blades -1 , 0 and $+1$

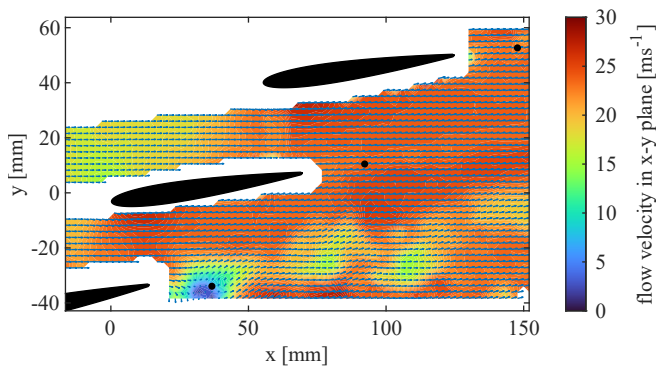
Fig. 9. Development of stall flutter after an impulse applied to blade -1 . Wind speed 20 ms^{-1} , $\text{AOA} -8^\circ$

In such measurements, PIV is an important tool to measure and visualise the flow through the blade cascade. For the above case, the PIV was set to observe the two channels between the oscillating blades and the wakes behind their trailing edges. Instantaneous snapshots from the developed flutter case at about $t = 2 \text{ s}$ are shown in Fig. 10, where the contour colours show the

velocity magnitude in the measurement plane and the arrows are the evaluated velocity vectors. The visible blades on the snapshots are the bottom left corner blades -1 , 0 and $+1$. The black points behind the trailing edges of the blades are positions where the flow velocity was observed and further investigated. The white areas are areas where the velocity could not be evaluated due to poor illumination (the illuminating laser was shining from the top right direction), camera lens perspective and low PIV resolution, which cannot capture the flow near the blade in such an overall view.



(a) At uppermost position of the blade -1 trailing edge



(b) While the trailing edge of the blade -1 moves downwards

Fig. 10. Instantaneous flow field snapshots during the flutter phase with velocity magnitude contours and velocity vectors evaluated from experimental PIV measurement

The first snapshot in Fig. 10a shows the situation when the trailing edge has reached its uppermost position. No flow separation is visible on the suction side of blades 0 and $+1$ and there is an accelerated flow in the first channel between blades -1 and 0 due to closing of the channel.

The second snapshot in Fig. 10b shows the situation 5ms after the first one in Fig. 10a, when the trailing edge of blade -1 started to move downwards. The velocity in the first channel decreased due to opening of the channel and vortex structures, caused by the flow separation, emerge from the suction side of the blade -1 . The periodic separation and re-attachment of the flow during blade oscillation is characteristic for the stall flutter.

5. CONCLUSION

This paper describes the design and development of an innovative experimental blade cascade for the study of stall flutter, operating in low subsonic flow conditions up to $Ma = 0.15$. It consists of five NACA 0010 prismatic blades with pitch degrees of freedom that can oscillate with amplitude up to 8° and frequency up to 60 Hz.

First, the geometry of the blade cascade was designed. In previous experiments, it had been impossible to achieve stall flutter at the inner blades of the cascade under any flow conditions. Due to narrow channels between the blades, the flow had been stabilised and flow separation had been suppressed. Therefore, numerical calculations and experimental tests were carried out to determine the appropriate blade spacing for stall to occur, and this geometry with increased spacing was used for the new cascade geometry design.

For accurate measurements, a completely new blade suspension system with moment and angular displacement sensors and excitation coils was designed. A flat spring suspension system with low damping was developed to support the blades and provide torsional stiffness, and aerodynamic moment measurement was achieved using a strain gauge moment sensor shaft. Excitation was provided by electromagnetic torsional shakers, which allowed not only harmonic moment excitation to perform parametric studies with different flow and blade oscillation parameters during controlled flutter experiments, but also pulse excitation.

Once manufactured, assembled and tuned, the capabilities of the new cascade were tested. Firstly, controlled flutter tests were carried out using both the TWM and AIC approaches. It was shown that the approximation of the cascade stability using the AIC approach is equivalent to the TWM approach for the three inner blades of the cascade within the limits where the electromagnetic excitation is able to enforce the controlled motion. Within those limits, the blade cascade is in classical flutter region with attached flow where the linear superposition principle can be applied. The resulting stability curves were evaluated for a wide range of flow and oscillation parameters, i.e. wind speed, AOA, oscillation frequency and amplitude, to identify the unstable regions.

In the next step, the cascade was brought to the edge of stability by setting the parameters based on the previously obtained stability curves, and the advantage of electromagnetic excitation was used to destabilise the cascade. Short moment pulses were applied to the individual blades and the response of the cascade was observed. The oscillation of the excited blade is transmitted through the cascade by the aeroelastic forces and either decays with time or triggers the stall flutter and the amplitudes of the oscillations increase. Capturing and analysing of this stall flutter initiation from a mechanical perspective by measuring the moments and displacements, and from a flow field perspective by incorporating the PIV measurement, provides valuable data for a basic understanding of the stall flutter phenomenon.

ACKNOWLEDGEMENTS

This work was supported by the research project of Czech science foundation No. 20-26779S “Study of dynamic stall flutter instabilities and their consequences in turbomachinery application by mathematical, numerical and experimental methods”.

REFERENCES

- [1] J.J. Waite, “Physical insights, steady aerodynamic effects, and a design tool for low-pressure turbine flutter,” Ph.D. dissertation, Department of Mechanical Engineering and Materials Science, Duke University, 2016.
- [2] D.M. Vogt and T.H. Fransson, “A new turbine cascade for aeromechanical testing,” in *Proceedings of the 16th Symposium on Measuring Techniques in Transonic and Supersonic Flow in Cascades and Turbomachines*, 2002.
- [3] C.S. Prasad and L. Pešek, “Efficient prediction of classical flutter stability of turbomachinery blade using the boundary element type numerical method,” *Eng. Anal. Bound. Elem.*, vol. 113, pp. 328–345, 2020.
- [4] M. Casoni and E. Benini, “A review of computational methods and reduced order models for flutter prediction in turbomachinery,” *Aerospace*, vol. 8, no. 9, p. 242, 2021.
- [5] J. Marshall and M. Imregun, “A review of aeroelasticity methods with emphasis on turbomachinery applications,” *J. Fluids Struct.*, vol. 10, no. 3, pp. 237–267, 1996.
- [6] L. Sbardella, A. Sayma, and M. Imregun, “Semi-structured meshes for axial turbomachinery blades,” *Int. J. Numer. Methods Fluids*, vol. 32, no. 5, pp. 569–584, 2000.
- [7] M. Imregun and M. Vahdati, “Aeroelasticity analysis of a bird-damaged fan assembly using a large numerical model,” *Aeronaut. J.*, vol. 103, no. 1030, pp. 569–578, 1999.
- [8] M. Vahdati, A. Sayma, M. Imregun, and G. Simpson, “Core-compressor rotating stall simulation with a multi-bladerow model,” in *Unsteady Aerodynamics, Aeroacoustics and Aeroelasticity of Turbomachines*, 2006, pp. 313–329.
- [9] F. Sisto, S. Thangam, and A. Abdel-Rahim, “Computational prediction of stall flutter in cascaded airfoils,” *AIAA J.*, vol. 29, no. 7, pp. 1161–1167, 1991.
- [10] V.I. Gnesin and Y.A. Bykov, “Numerical studies on aeroelastic characteristics of the turbomachine blade cascade operating under abnormal conditions,” *Probl. Mashinostr.*, vol. 7, no. 1, pp. 31–40, 2004.
- [11] V.I. Gnesin and L.V. Kolodyzhnaya, “Numerical simulation of the aeroelastic state of the vibrating turbomachine blade cascade in the three-dimensional transonic nonviscous gas flow,” *Probl. Mashinostr.*, vol. 1, pp. 65–76, 1998.
- [12] R. Rządkowski, V.I. Gnesin, and L. Kolodyzhnaya, “3d viscous flutter of 11th configuration blade row,” *Adv. Vibr. Eng.*, vol. 8, no. 3, pp. 213–221, 07 2009.
- [13] N. Gourdain, F. Sicot, F. Duchaine, and L. Gicquel, “Large eddy simulation of flows in industrial compressors: a path from 2015 to 2035,” *Philos. Trans. R. Soc. A-Math. Phys. Eng. Sci.*, vol. 372, no. 2022, p. 20130323, 2014.
- [14] A. Pajak and R. Rządkowski, “Influence of mesh density and turbulence models on 2d viscous flutter in 11th standard configuration,” in *Turbo Expo: Power for Land, Sea, and Air*, vol. 44731, 2012, pp. 1431–1439.
- [15] M. Nakhchi and M. Rahmati, “Direct numerical simulations of flutter instabilities over a vibrating turbine blade cascade,” *J. Fluids Struct.*, vol. 104, p. 103324, 2021, doi: [10.1016/j.jfluidstructs.2021.103324](https://doi.org/10.1016/j.jfluidstructs.2021.103324).
- [16] S.W. Naung, M.E. Nakhchi, and M. Rahmati, “Prediction of flutter effects on transient flow structure and aeroelasticity of low-pressure turbine cascade using direct numerical simulations,” *Aerospace Sci. Technol.*, vol. 119, p. 107151, 2021, doi: [10.1016/j.ast.2021.107151](https://doi.org/10.1016/j.ast.2021.107151).
- [17] C.S. Prasad and L. Pešek, “Analysis of classical flutter in steam turbine blades using reduced order aeroelastic model,” *MATEC Web Conf.*, vol. 211, p. 15001, 2018.
- [18] C.S. Prasad, P. Šnábl, and L. Pešek, “A meshless method for subsonic stall flutter analysis of turbomachinery 3d blade cascade,” *Bull. Pol. Acad. Sci. Tech. Sci.*, vol. 69, no. 6, p. e139000, 2021, doi: [10.24425/bpasts.2021.139000](https://doi.org/10.24425/bpasts.2021.139000).
- [19] C.S. Prasad, R. Kolman, and L. Pešek, “Meshfree reduced order model for turbomachinery blade flutter analysis,” *Int. J. Mech. Sci.*, vol. 222, p. 107222, 2022.
- [20] C.S. Prasad and L. Pešek, “Classical flutter study in turbomachinery cascade using boundary element method for incompressible flows,” in *Advances in Mechanism and Machine Science: Proceedings of the 15th IFToMM World Congress on Mechanism and Machine Science 15*, 2019, pp. 4055–4064.
- [21] V. Sláma, B. Rudas, J. Ira, A. Macálka, P. Eret, and V. Tsybalyuk, “The validation of flutter prediction in a linear cascade of non-rigid turbine blades,” in *Turbo Expo: Power for Land, Sea, and Air*, vol. 51159, 2018, p. V07CT36A010.
- [22] F.O. Carta and A.O. St. Hilaire, “Experimentally determined stability parameters of a subsonic cascade oscillating near stall,” *J. Eng. Gas Turbines Power*, vol. 100, no. 1, pp. 111–120, 1978, doi: [10.1115/1.3446301](https://doi.org/10.1115/1.3446301).
- [23] F.O. Carta and A.O. St. Hilaire, “Effect of interblade phase angle and incidence angle on cascade pitching stability,” *J. Eng. Gas Turbines Power*, vol. 102, no. 2, pp. 391–396, 1980, doi: [10.1115/1.3230268](https://doi.org/10.1115/1.3230268).
- [24] A. Bölcs and T. H. Fransson, “Aeroelasticity in turbomachines. comparison of theoretical and experimental cascade results.” 1986, technical Report, Ecole Polytechnique Federale de Lausanne, Lab de Thermique Appliquee.
- [25] H. Körbächer and A. Bölcs, “Experimental investigation of the unsteady behavior of a compressor cascade in an annular ring channel,” in *Proceedings of the 7th International Symposium on Unsteady Aerodynamics and Aeroelasticity of Turbomachinery*, 1994.
- [26] J. Lepicovsky, E. R. McFarland, V. R. Capece, T. A. Jett, and R. G. Senyitko, “Methodology of blade unsteady pressure measurement in the nasa transonic flutter cascade,” 2002, nASA Technical Memorandum 211894.
- [27] H. Yang and L. He, “Experimental investigation of linear compressor cascade with three-dimensional blade oscillation,” *J. Propuls. Power*, vol. 20, no. 1, pp. 180–188, 2004.
- [28] P. Šidlof, D. Šimurda, J. Lepicovsky, M. Štěpán, and V. Vomáčko, “Flutter in a simplified blade cascade: Limits of the quasi-steady approximation,” *J. Fluids Struct.*, vol. 120, p. 103913, 2023, doi: [10.1016/j.jfluidstructs.2023.103913](https://doi.org/10.1016/j.jfluidstructs.2023.103913).

- [29] P. Eret and V. Tsybalyuk, "Experimental Subsonic Flutter of a Linear Turbine Blade Cascade With Various Mode Shapes and Chordwise Torsion Axis Locations," *J. Turbomach.*, vol. 145, no. 6, p. 061002, 2022, doi: [10.1115/1.4056204](https://doi.org/10.1115/1.4056204).
- [30] A. Stelmakh, "Stability limits of gte axial compressor blade rings for subsonic bending-torsion cascade flutter on stalling and non-stalling flow," *Strength Mater.*, pp. 1–10, 2023, doi: [10.1007/s11223-023-00522-7](https://doi.org/10.1007/s11223-023-00522-7).
- [31] J. Lepicovsky, P. Šidlof, D. Šimurda, M. Štěpán, and M. Luxa, "New test facility for forced blade flutter research," *AIP Conf. Proc.*, vol. 2323, no. 1, p. 030001, 2021, doi: [10.1063/5.0041990](https://doi.org/10.1063/5.0041990).
- [32] M. Keerthi and A. Kushari, "Experimental study of aerodynamic damping of an annular compressor cascade with large mean incidences," *J. Turbomach.*, vol. 141, no. 6, p. 061002, 2019, doi: [10.1115/1.4042214](https://doi.org/10.1115/1.4042214).
- [33] V.A. Tsimbalyuk, "Method of measuring transient aerodynamic forces and moments on a vibrating cascade," *Strength Mater.*, vol. 28, pp. 150–157, 1996, doi: [10.1007/BF02215842](https://doi.org/10.1007/BF02215842).
- [34] V. Tsimbalyuk, A. Zinkovskii, V. Gnesin, R. Rzadkowski, and J. Sokolowski, *Experimental and numerical investigation of 2D palisade flutter for the harmonic oscillations*. Springer Netherlands, 2006, pp. 53–63.
- [35] V. Sláma *et al.*, "Experimental and numerical study of controlled flutter testing in a linear turbine blade cascade," *Acta Polytechnica CTU Proc.*, vol. 20, pp. 98–107, 2018, doi: [10.14311/APP.2018.20.0098](https://doi.org/10.14311/APP.2018.20.0098).
- [36] P. Jutur and R.N. Govardhan, "Flutter in Started and Unstarted Transonic Linear Cascades: Simultaneous Measurements of Unsteady Loads and Shock Dynamics," *J. Turbomach.*, vol. 141, no. 12, p. 121004, 2019, doi: [10.1115/1.4045105](https://doi.org/10.1115/1.4045105).
- [37] K. Vogel, A.D. Naidu, and M. Fischer, "Comparison of the influence coefficient method and travelling wave mode approach for the calculation of aerodynamic damping of centrifugal compressors and axial turbines," in *Proceedings of ASME Turbo Expo 2017: Turbomachinery Technical Conference and Exposition*, 2017, doi: [10.1115/GT2017-64643](https://doi.org/10.1115/GT2017-64643).
- [38] Y. Hanamura, H. Tanaka, and K. Yamaguchi, "A simplified method to measure unsteady forces acting on the vibrating blades in cascade," *Bull. JSME*, vol. 23, no. 180, pp. 880–887, 1980, doi: [10.1299/jsme1958.23.880](https://doi.org/10.1299/jsme1958.23.880).
- [39] F.O. Carta, "Coupled blade-disk-shroud flutter instabilities in turbojet engine rotors," *J. Eng. Power*, vol. 89, no. 3, pp. 419–426, 1967, doi: [10.1115/1.3616708](https://doi.org/10.1115/1.3616708).
- [40] M. May, Y. Mauffrey, and F. Sicot, "Numerical flutter analysis of turbomachinery bladings based on time-linearized, time-spectral and time-accurate simulations," in *IFASD 2011 – 15th International Forum on Aeroelasticity and Structural Dynamics*, 2011.
- [41] F.O. Carta, "An experimental investigation of gapwise periodicity and unsteady aerodynamic response in an oscillating cascade," 1982, NASA Contractor Report 3513.
- [42] P. Šnábl, L. Pešek, C. S. Prasad, and P. Procházka, "Experimental investigation of classical flutter in blade cascade," in *IFASD 2022 – International Forum on Aeroelasticity and Structural Dynamics*, 2022.
- [43] P. Šnábl, L. Pešek, C. S. Prasad, and S. Chindada, "Problematics of aerodynamic damping calculation from measured data of 5-blade cascade," in *CM 2022 – 37th conference with international participation Computational Mechanics*, 2022.
- [44] J. Horáček, J. Kozánek, and J. Veselý, "Dynamic and stability properties of the aeroelastic model," *Eng. Mech.*, vol. 11, 2005, in Czech.
- [45] V. Vlček and M. Luxa, "Preliminary aeroelastic experiments on the profile with two degrees of freedom," *Eng. Mech.*, vol. 11, 2005, in Czech.
- [46] V. Vlček, I. Zolotarev, and J. Kozánek, "Aerodynamic forces measured on a fluttering profile," *Eng. Mech.*, vol. 21, no. 2, pp. 91–96, 2014.
- [47] J. Kozánek, V. Vlček, and I. Zolotarev, "Vibrating profile in the aerodynamic tunnel – identification of the start of flutter," *J. Appl. Nonlinear Dyn.*, vol. 3, no. 4, pp. 317–323, 2014, doi: [10.5890/JAND.2014.12.003](https://doi.org/10.5890/JAND.2014.12.003).
- [48] V. Vlček and P. Procházka, "Test section of the wind tunnel for aeroelastic experiments with blade cascades," *EPJ Web Conf.*, vol. 213, p. 02095, 2019, doi: [10.1051/epjconf/201921302095](https://doi.org/10.1051/epjconf/201921302095).
- [49] J. Vimmr, O. Bublík, A. Pecka, and L. Pešek, "Numerical analysis of flutter instability in simplified blade cascade," *Eccomas Proceedia COMPdyn*, pp. 3795–3807, 2017, doi: [10.7712/120117.5685.17525](https://doi.org/10.7712/120117.5685.17525).
- [50] J. Vimmr, O. Bublík, H. Prausová, J. Hála, and L. Pešek, "Numerical simulation of fluid flow through simplified blade cascade with prescribed harmonic motion using discontinuous galerkin method," *EPJ Web Conf.*, vol. 180, p. 02117, 2018, doi: [10.1051/epjconf/201818002117](https://doi.org/10.1051/epjconf/201818002117).
- [51] J. Vimmr, O. Bublík, A. Pecka, L. Pešek, and P. Procházka, "Numerical and experimental study of fluid flow in simplified blade cascade with prescribed harmonic motion," *EPJ Web Conf.*, vol. 180, p. 02116, 2018, doi: [10.1051/epjconf/201817002116](https://doi.org/10.1051/epjconf/201817002116).
- [52] P. Procházka, V. Uruba, L. Pešek, and V. Bula, "On the effect of moving blade grid on the flow field characteristics," *EPJ Web Conf.*, vol. 180, p. 02086, 2018, doi: [10.1051/epjconf/201818002086](https://doi.org/10.1051/epjconf/201818002086).
- [53] L. Pešek *et al.*, "Aero-elastic couplings and dynamic behaviour of rotational periodic bodies - description of the grant gacr 16-04546s solution in 2017," 2017, research Report, Institute of Thermomechanics of the CAS, no. Z1578/17.
- [54] P. Šnábl, L. Pešek, C.S. Prasad, V. Bula, and J. Cibulka, "Experimental setup and measurement for evaluation of blade cascade stall flutter instability," in *ICSV 2021 – 27th International Congress on Sound and Vibration*, 2021.